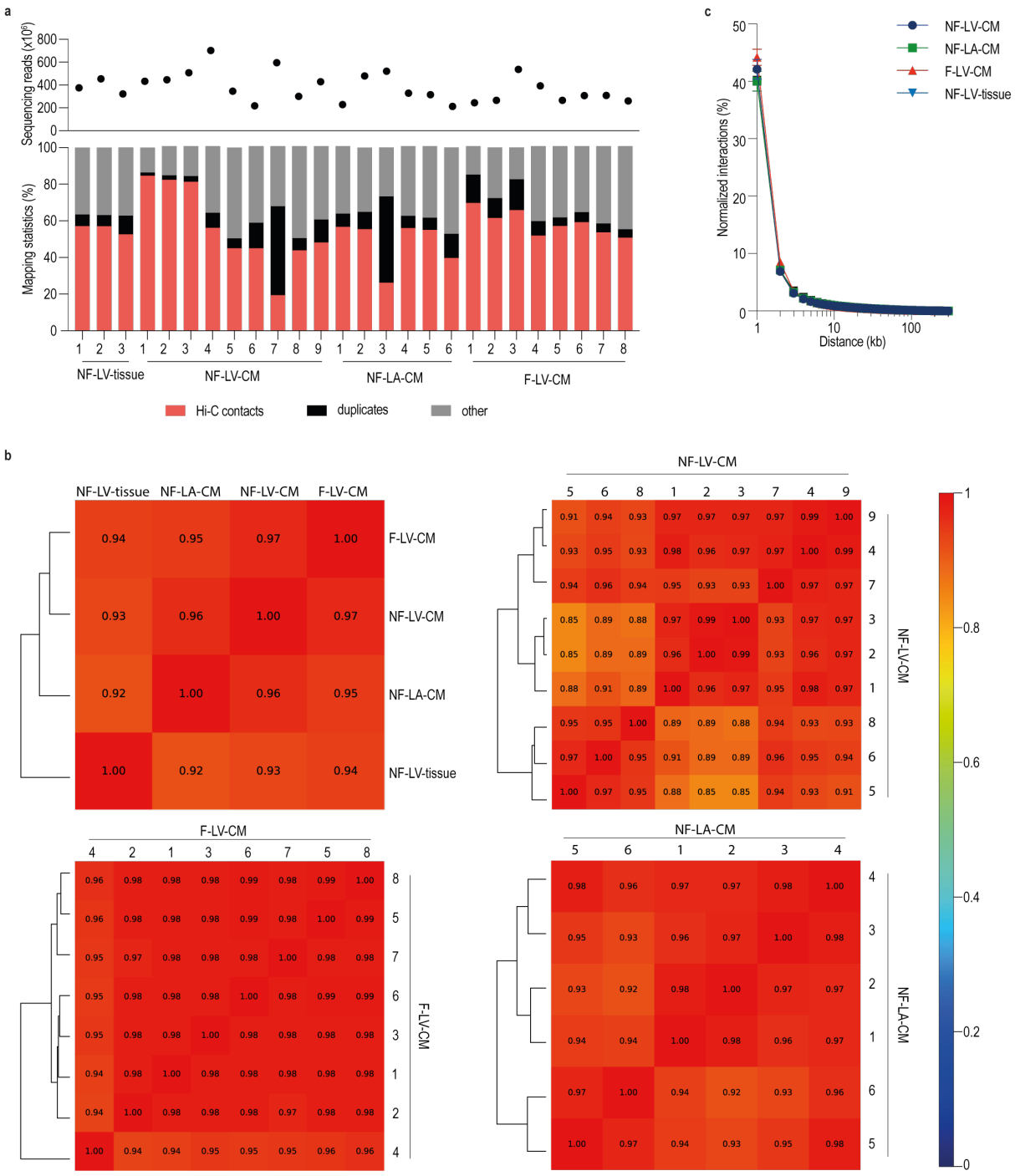

Supplementary Fig.1: Quality and correlation of Hi-C sequencing reads obtained from different biological replicates.
a Sequencing and mapping statistics of Hi-C data.
b Heatmaps of Spearman correlation coefficients of genome-wide Hi-C reads for the different biological replicates at 100 kb resolution.
c Line plot of genomic distance versus contact counts using 100 kb resolution Hi-C matrices.

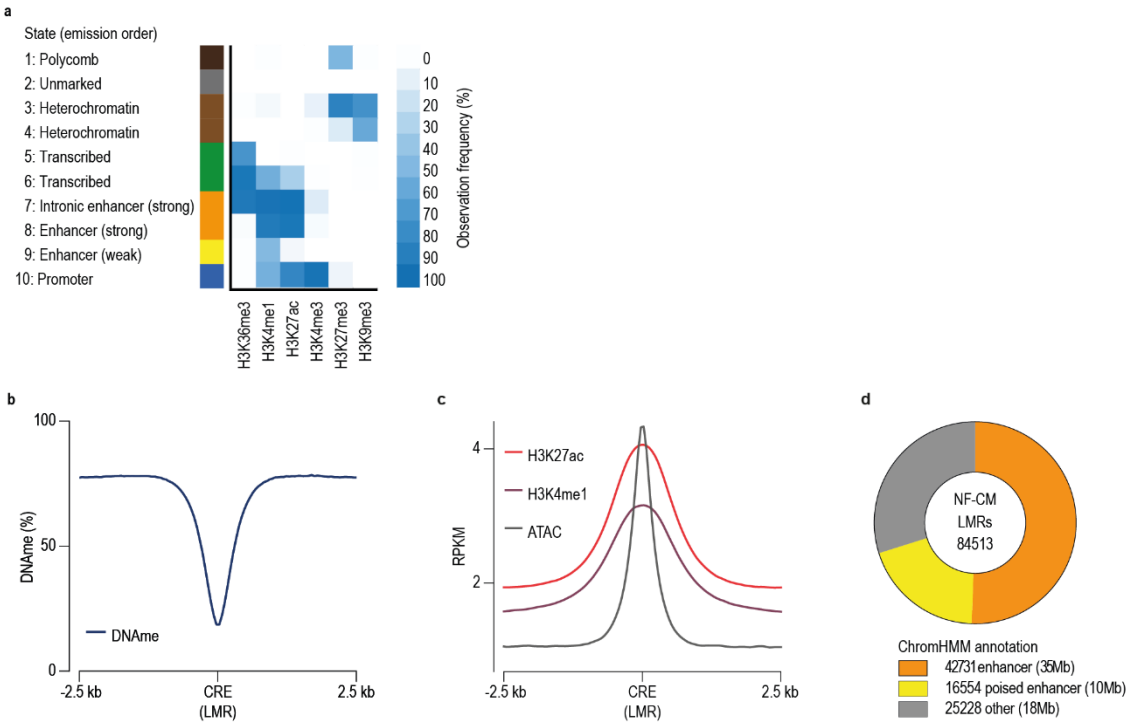

Supplementary Fig. 2: Chromatin state of LMRs

a Chromatin states were learned using a multi variant hidden Markov model based on genome wide occurrence of combinations of different histone marks (ChromHMM). Shown is a frequency heatmap.

b,c Profiles of CpG methylation (b, %), histone modifications and chromatin accessibility (c, enrichment) flanking the LMR centers of NF-LV-CM.

d LMRs detected in NF-LV-CM were categorized into enhancers, poised enhancers and other chromatin states according to the ChromHMM model (see a). Shown is the number of LMRs for each category and the genomic length is annotated.

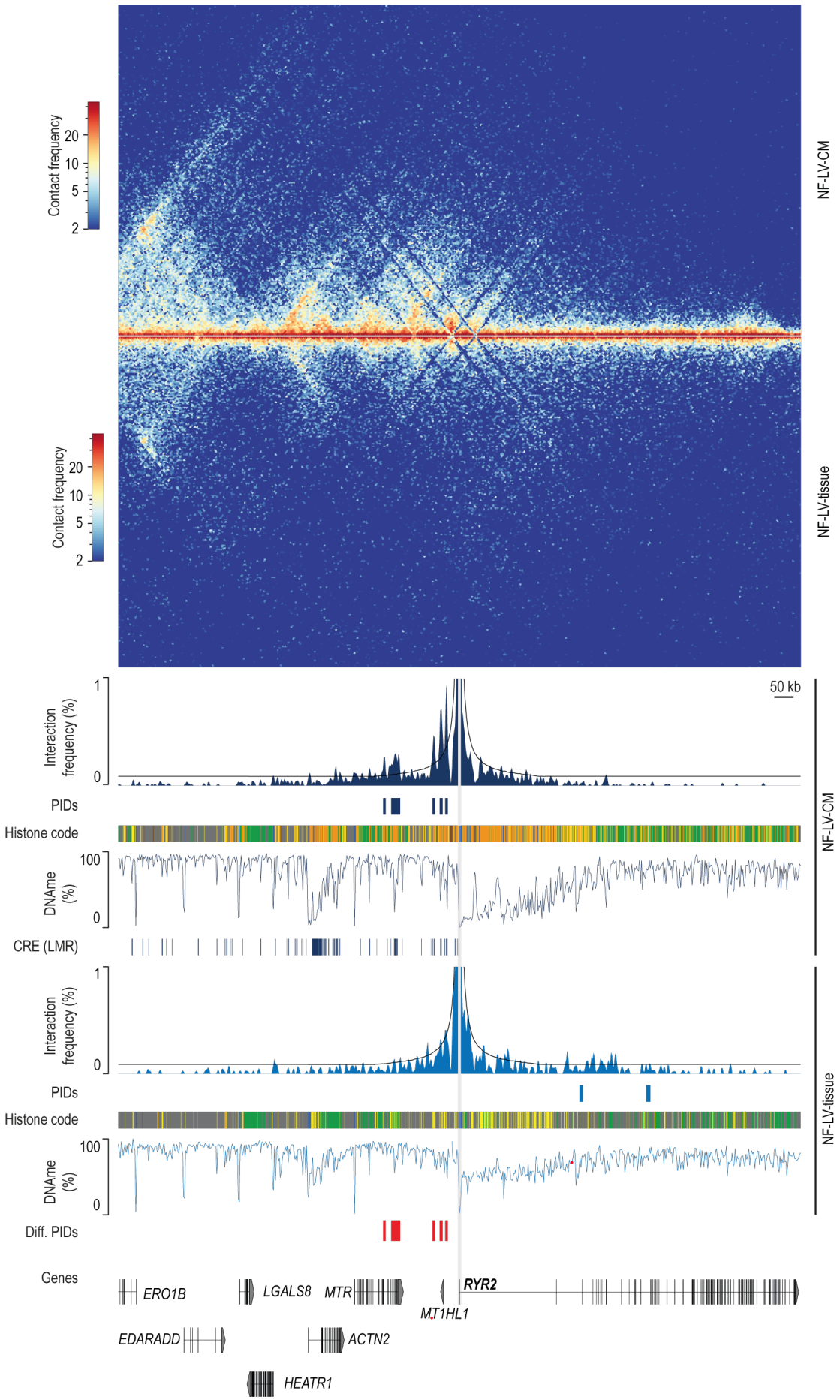
Contact frequency
20
10
5
2
NF-LV-CM
Contact frequency
20
10
5
2
NF-LV-tissue
50 kb
Interaction frequency (%)
1
0
PIDs
Histone code
DNAme (%)
100
0
CRE (LMR)
NF-LV-CM
Interaction frequency (%)
1
0
PIDs
Histone code
DNAme (%)
100
0
Diff. PIDs
NF-LV-tissue
Genes
ERO1B
LGALS8
MTR
RYR2
MT1HL1
EDARADD
ACTN2
HEATR1

Supplementary Fig. 3: Comparison of cardiac tissue and CM chromatin interactions for the *RYR2* locus.
Original traces of and histone marks (ChromHMM), virtual viewpoint analysis of *RYR2* promoter interactions (Hi-C), and mCpG (DNA methylation sequencing). Low-methylated regions (LMR), PIDs, and differential PIDs are annotated. Hi-C data derived from *n* biological replicates: NF-LV-CM, 3; NF-LV-CN, 3. CRE, *cis*-regulatory elements. Diff. PIDs, Differential promoter-interacting domains.

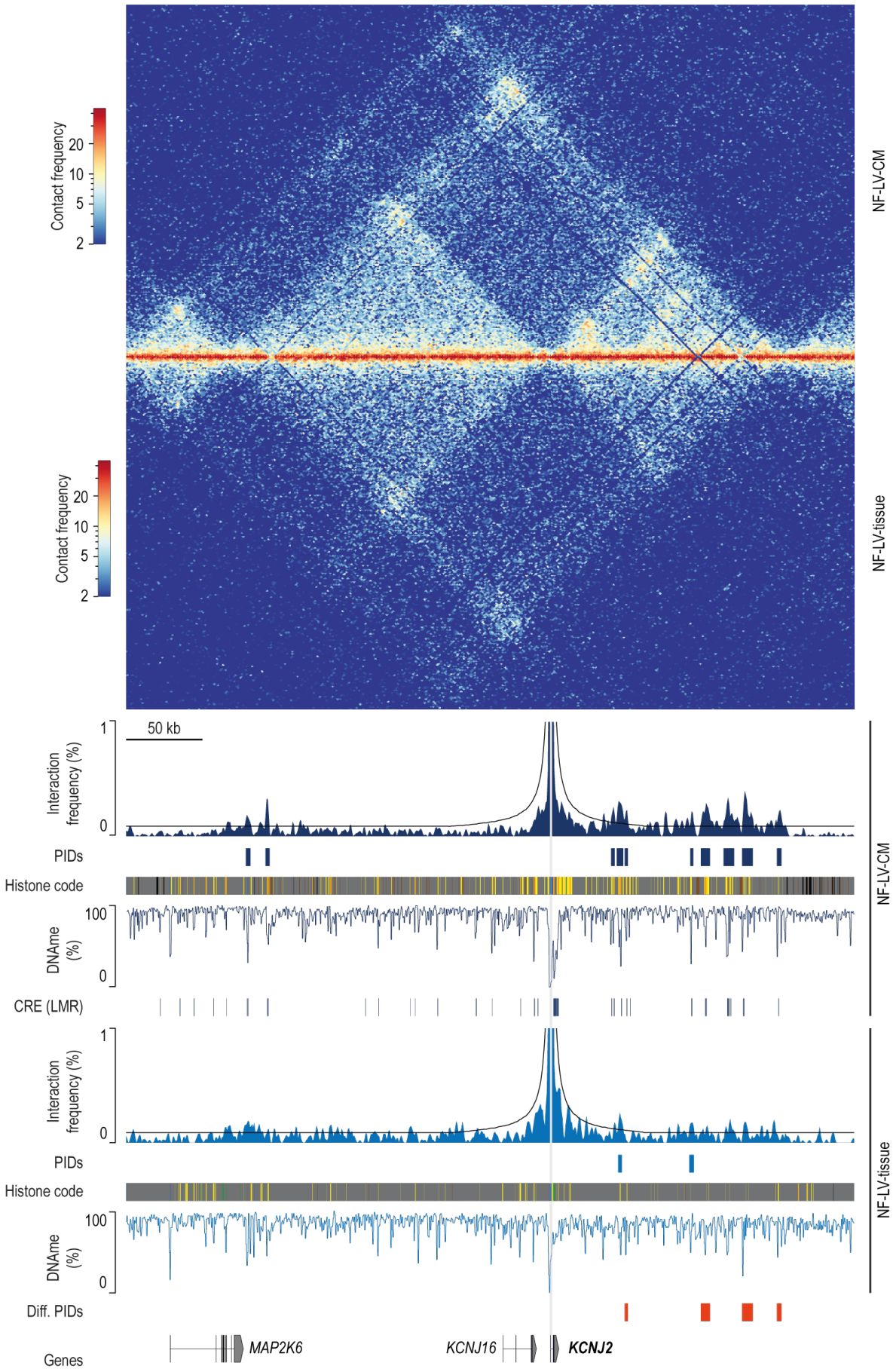
Contact frequency
20
10
5
2
NF-LV-CM
Contact frequency
20
10
5
2
NF-LV-tissue
50 kb
Interaction frequency (%)
1
0
PIDs
Histone code
DNAme (%)
100
0
CRE (LMR)
NF-LV-CM
Interaction frequency (%)
1
0
PIDs
Histone code
DNAme (%)
100
0
Diff. PIDs
NF-LV-tissue
Genes
MAP2K6
KCNJ16
KCNJ2

Supplementary Fig. 4: Comparison of cardiac and CM chromatin interactions for the *KCNJ2* locus.
see legend Supplementary Fig. 3

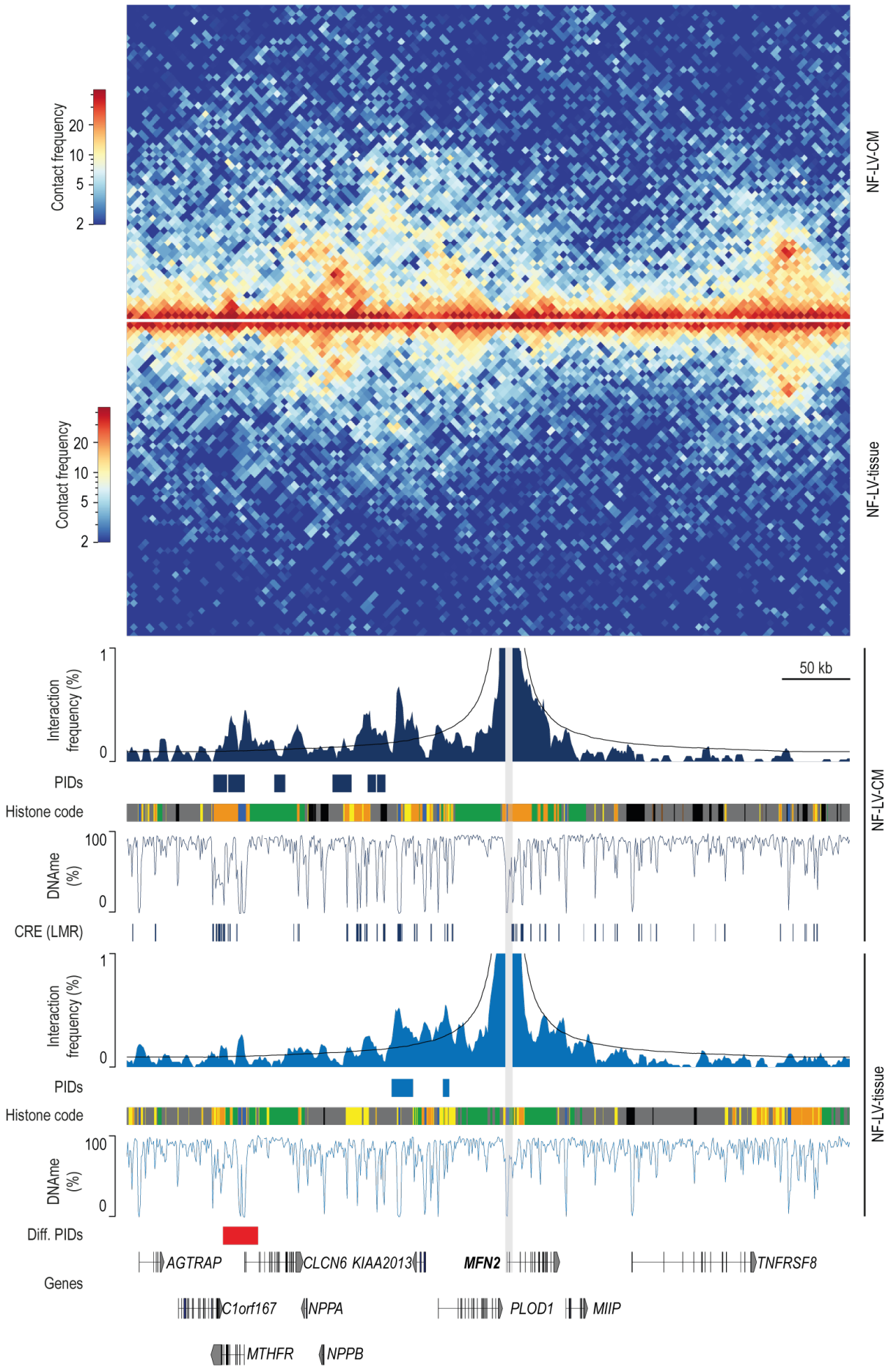
Contact frequency
20
10
5
2
NF-LV-CM
Contact frequency
20
10
5
2
NF-LV-tissue
Interaction frequency (%)
1
0
50 kb
PIDs
Histone code
DNAme (%)
100
0
CRE (LMR)
NF-LV-CM
Interaction frequency (%)
1
0
PIDs
Histone code
DNAme (%)
100
0
NF-LV-tissue
Diff. PIDs
Genes
AGTRAP
CLCN6 KIAA2013
MFN2
TNFRSF8
C1orf167
NPPA
PLOD1
MIIP
MTHFR
NPPB

Supplementary Fig. 5: Comparison of cardiac and CM chromatin interactions for the *MFN2* locus.
see legend Supplementary Fig. 3

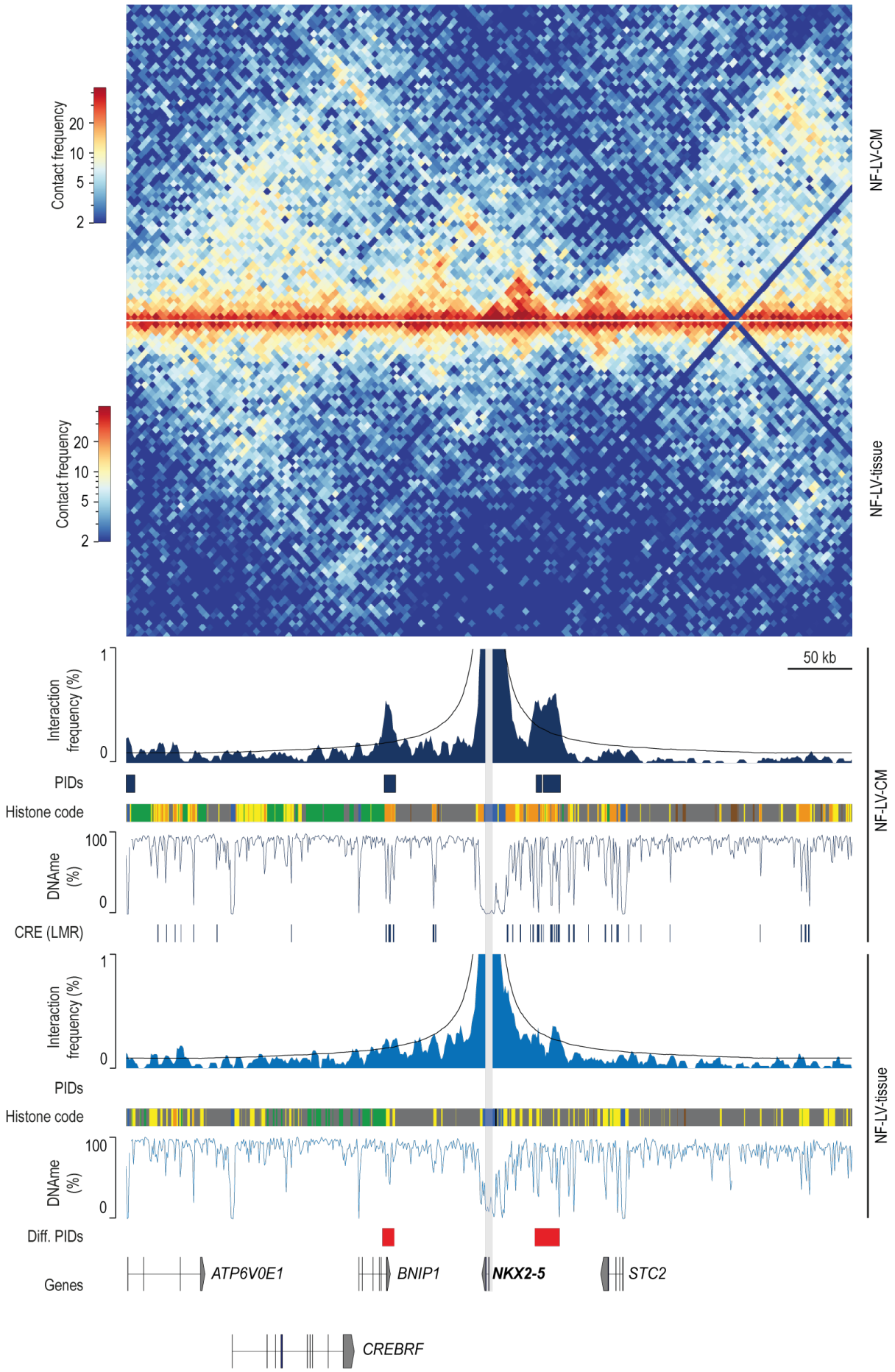
Contact frequency
20
10
5
2
NF-LV-CM
Contact frequency
20
10
5
2
NF-LV-tissue
Interaction frequency (%)
1
0
50 kb
PIDs
Histone code
DNAme (%)
100
0
CRE (LMR)
NF-LV-CM
Interaction frequency (%)
1
0
PIDs
Histone code
DNAme (%)
100
0
Diff. PIDs
NF-LV-tissue
Genes
ATP6V0E1
BNIP1
NKX2-5
STC2
CREBRF

Supplementary Fig. 6: Comparison of cardiac and CM chromatin interactions for the *NKX2-5* locus.
see legend Supplementary Fig. 3

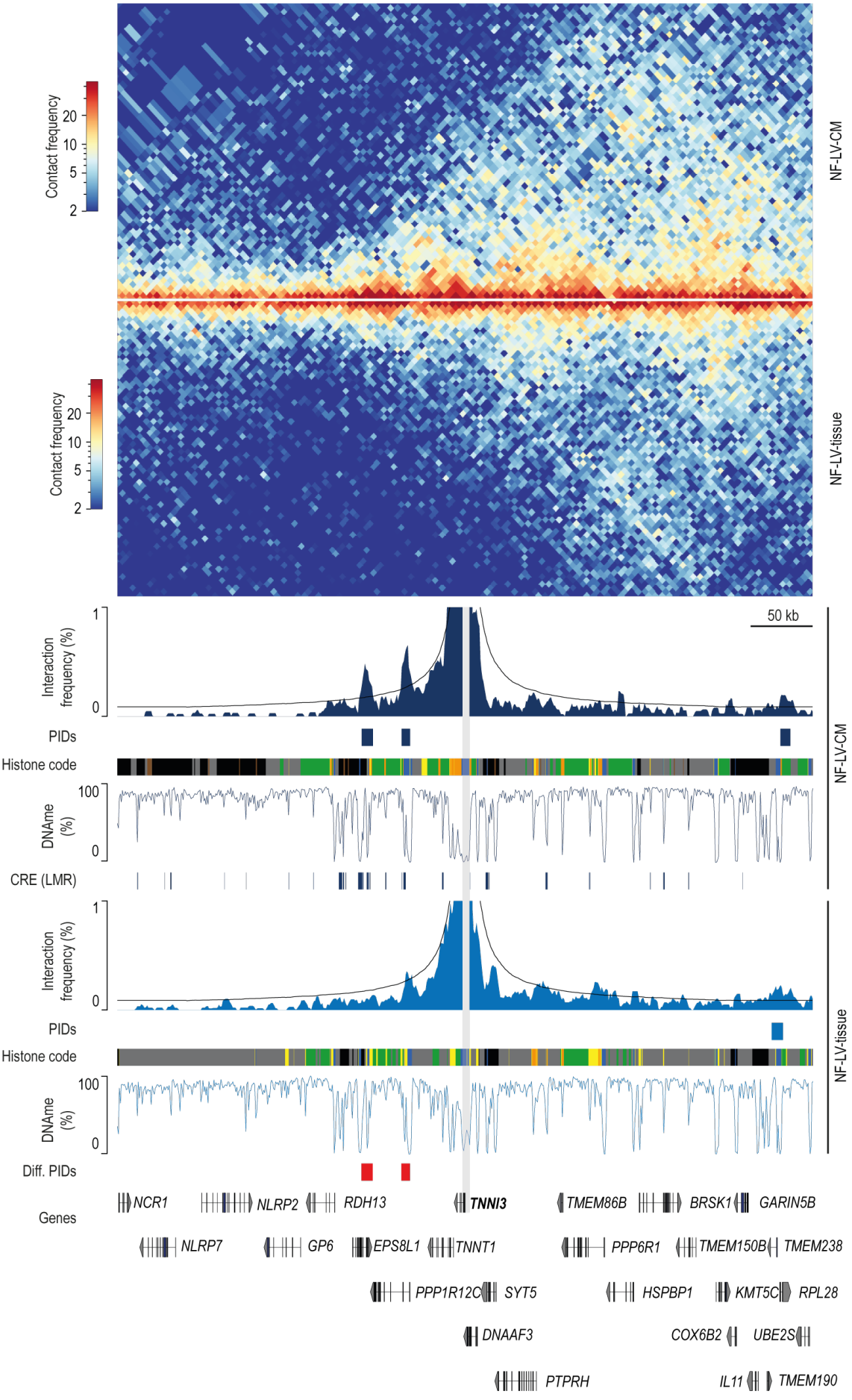
Contact frequency
20
10
5
2
NF-LV-CM
Contact frequency
20
10
5
2
NF-LV-tissue
50 kb
Interaction frequency (%)
1
0
PIDs
Histone code
DNAme (%)
100
0
CRE (LMR)
NF-LV-CM
Interaction frequency (%)
1
0
PIDs
Histone code
DNAme (%)
100
0
Diff. PIDs
NF-LV-tissue
Genes
NCR1
NLRP2
RDH13
TNNI3
TMEM86B
BRSK1
GARIN5B
NLRP7
GP6
EPS8L1
TNNT1
PPP6R1
TMEM150B
TMEM238
PPP1R12C
SYT5
HSPBP1
KMT5C
RPL28
DNAAF3
COX6B2
UBE2S
PTPRH
IL11
TMEM190

Supplementary Fig. 7: Comparison of cardiac and CM chromatin interactions for the *TNNI3* locus.
see legend Supplementary Fig. 3

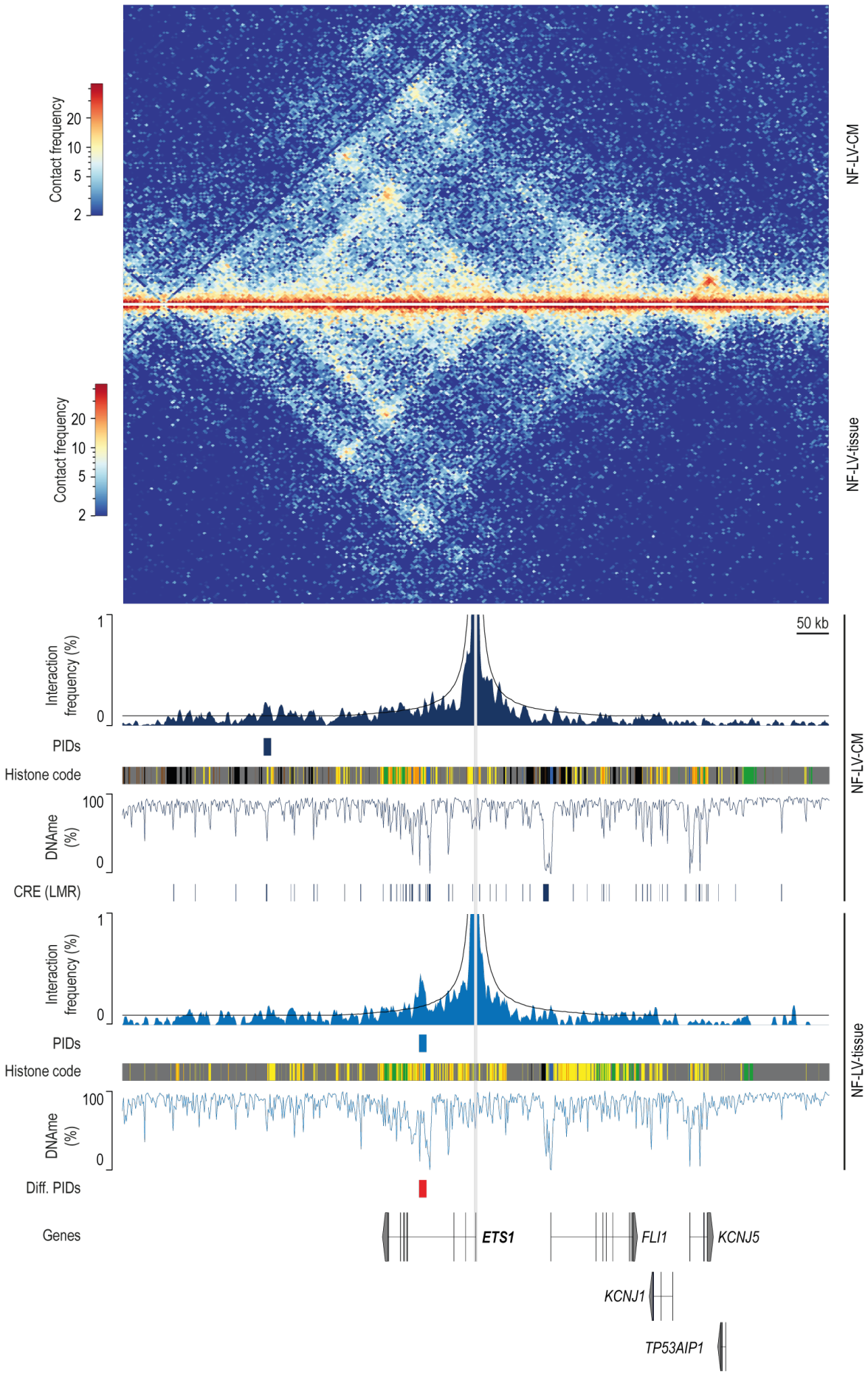
Contact frequency
20
10
5
2
NF-LV-CM
Contact frequency
20
10
5
2
NF-LV-tissue
Interaction frequency (%)
1
0
50 kb
PIDs
Histone code
DNAme (%)
100
0
CRE (LMR)
NF-LV-CM
Interaction frequency (%)
1
0
PIDs
Histone code
DNAme (%)
100
0
Diff. PIDs
NF-LV-tissue
Genes
ETS1
FLI1
KCNJ5
KCNJ1
TP53AIP1

Supplementary Fig. 8: Comparison of cardiac and CM chromatin interactions for the *ETS1* locus.
see legend Supplementary Fig. 3

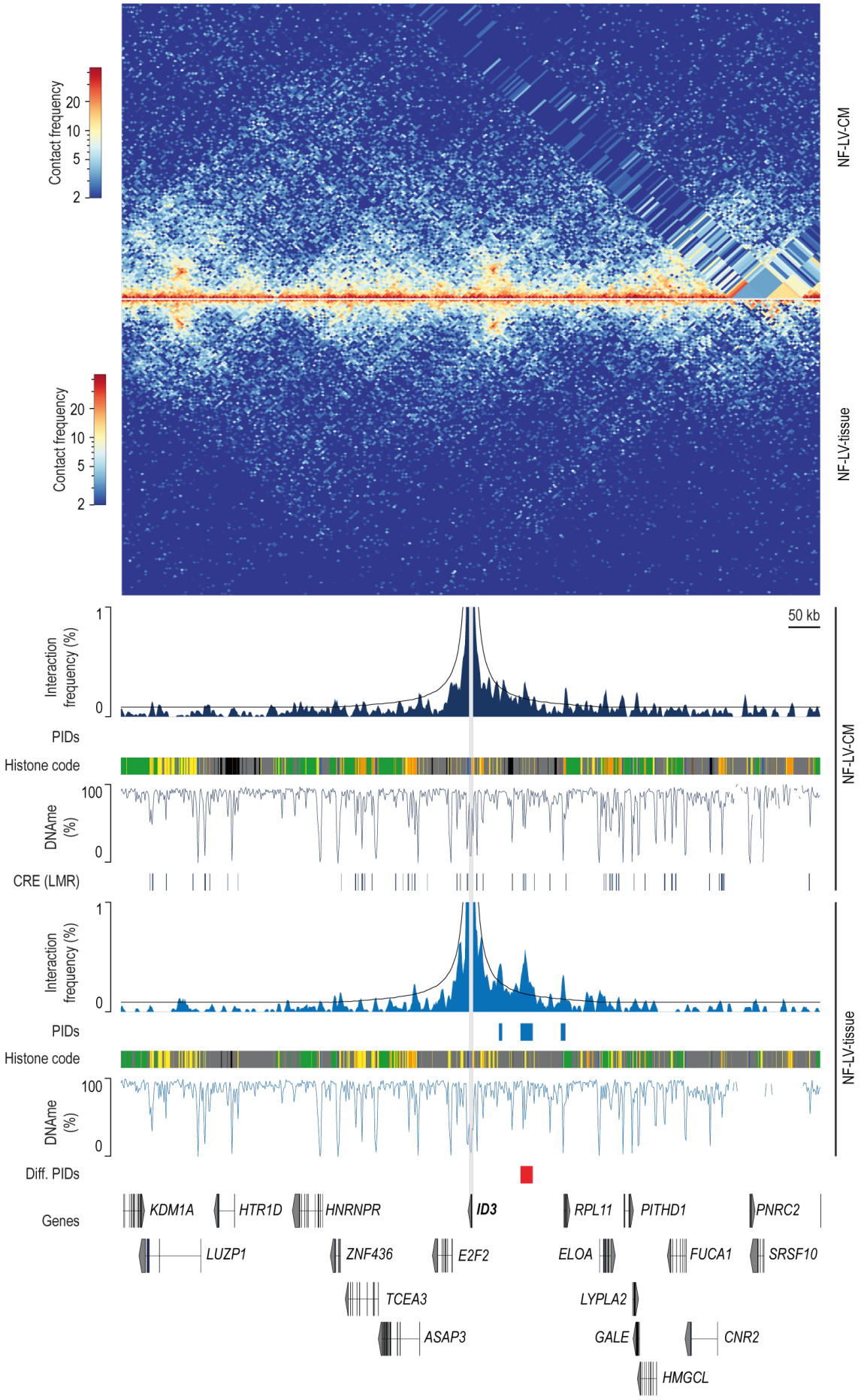
Contact frequency
20
10
5
2
NF-LV-CM
Contact frequency
20
10
5
2
NF-LV-tissue
50 kb
Interaction frequency (%)
1
0
PIDs
Histone code
DNAme (%)
100
0
CRE (LMR)
NF-LV-CM
Interaction frequency (%)
1
0
PIDs
Histone code
DNAme (%)
100
0
Diff. PIDs
NF-LV-tissue
Genes
KDM1A
HTR1D
HNRNPR
ID3
RPL11
PITHD1
PNRC2
LUZP1
ZNF436
E2F2
ELOA
FUCA1
SRSF10
TCEA3
LYPLA2
ASAP3
GALE
CNR2
HMGCL

Supplementary Fig. 9: Comparison of cardiac and CM chromatin interactions for the *ID3* locus.
see legend Supplementary Fig. 3

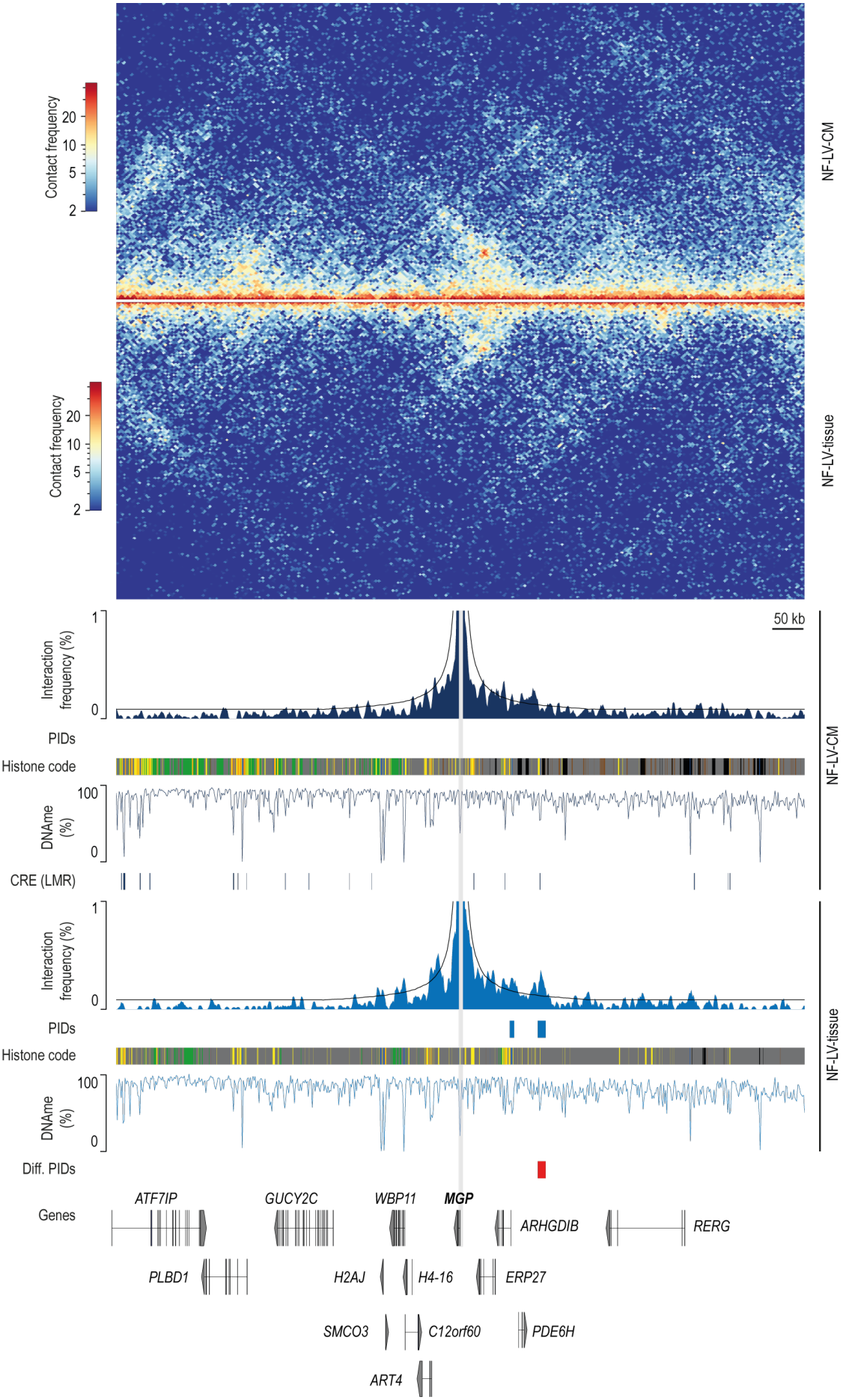
Contact frequency
20
10
5
2
NF-LV-CM
Contact frequency
20
10
5
2
NF-LV-tissue
50 kb
Interaction frequency (%)
1
0
PIDs
Histone code
DNAme (%)
100
0
CRE (LMR)
NF-LV-CM
Interaction frequency (%)
1
0
PIDs
Histone code
DNAme (%)
100
0
Diff. PIDs
NF-LV-tissue
Genes
ATF7IP
GUCY2C
WBP11
MGP
ARHGDIB
RERG
PLBD1
H2AJ
H4-16
ERP27
SMCO3
C12orf60
PDE6H
ART4

Supplementary Fig. 10: Comparison of cardiac and CM chromatin interactions for the *MGP* locus.
see legend Supplementary Fig. 3

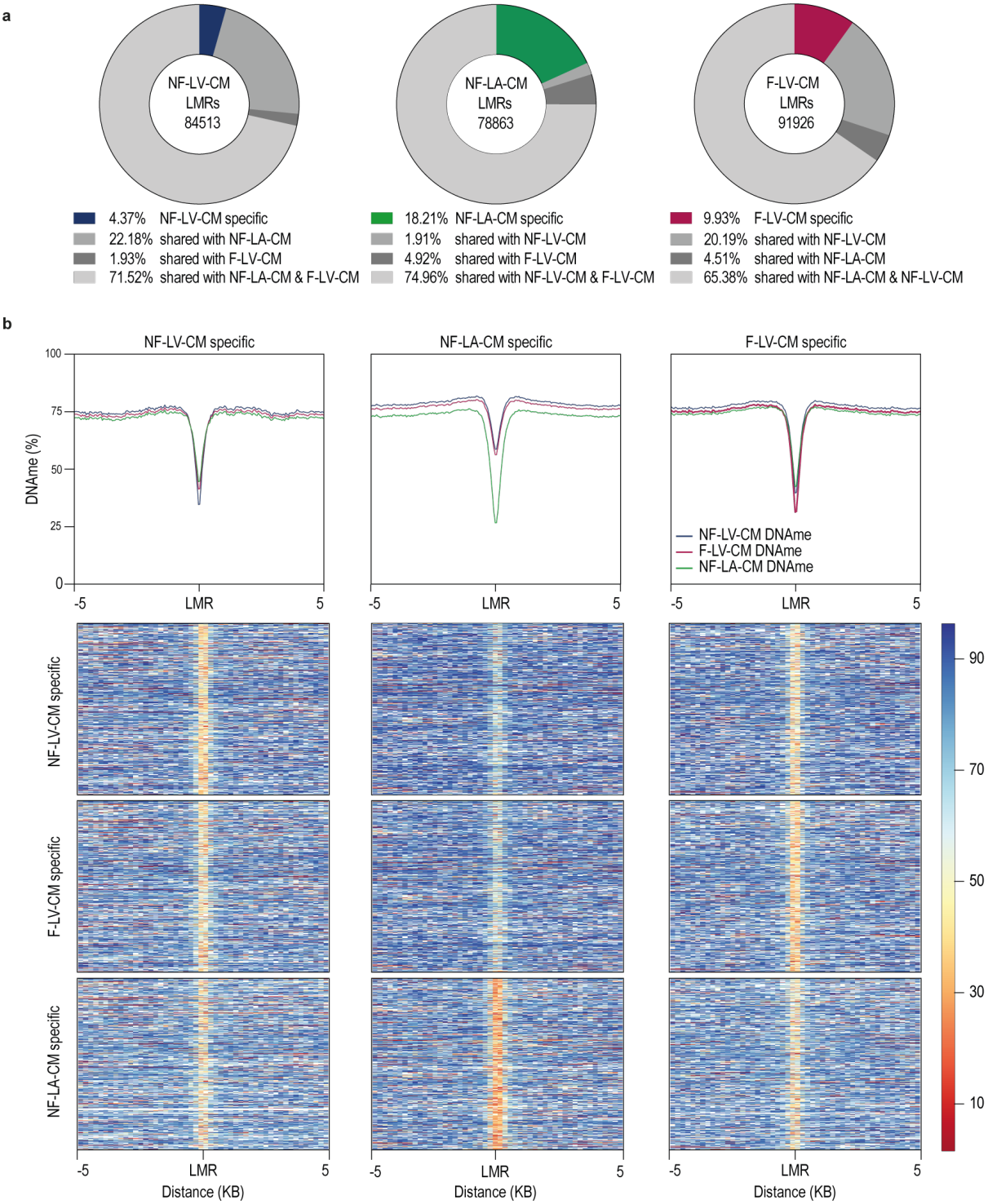

Supplementary Fig.11: Overlap between LMRs of NF-LV-CM, NF-LA-CM, and F-LV-CM.

a Pie charts highlight LMRs overlap between LMRs of NF-LV-CM, NF-LA-CM, and F-LV-CM.

b Average plots and heatmaps of mCpG are shown for LMRs for NF-LV-CM, NF-LA-CM, and F-LV-CM.

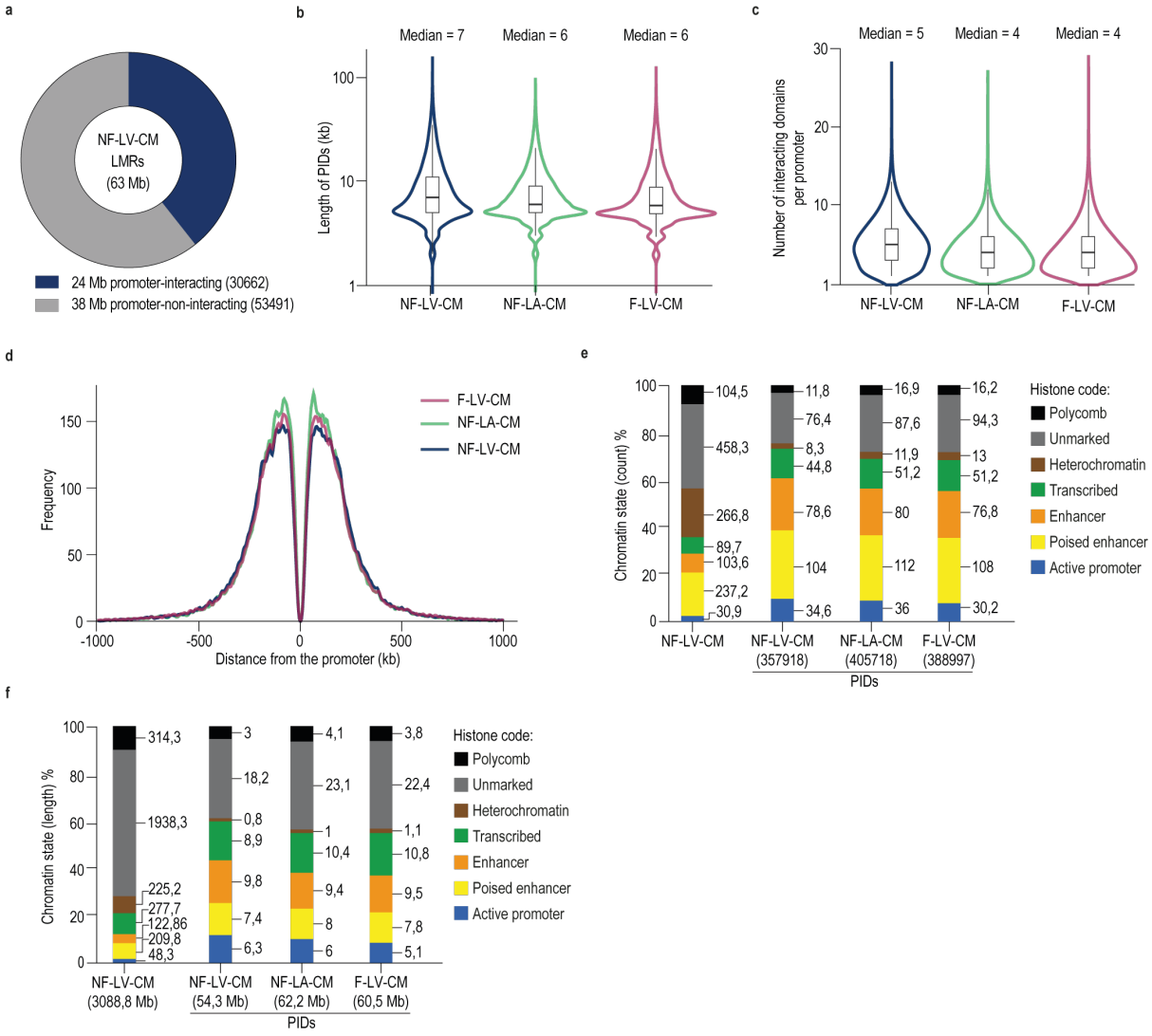

Supplementary Fig.12: Characterization of PIDs.

a Pie chart highlights the overlap between LMRs and PIDs of NF-LV-CM.

b,c Violin and box plots of length (b) and count (c) of PIDs of NF-LV-CM, NF-LA-CM, and F-LV-CM.

d Histogram of the PIDs' distance from the promoter.

e,f Percentage of histone codes identified using ChromHMM in human genome and PIDs.

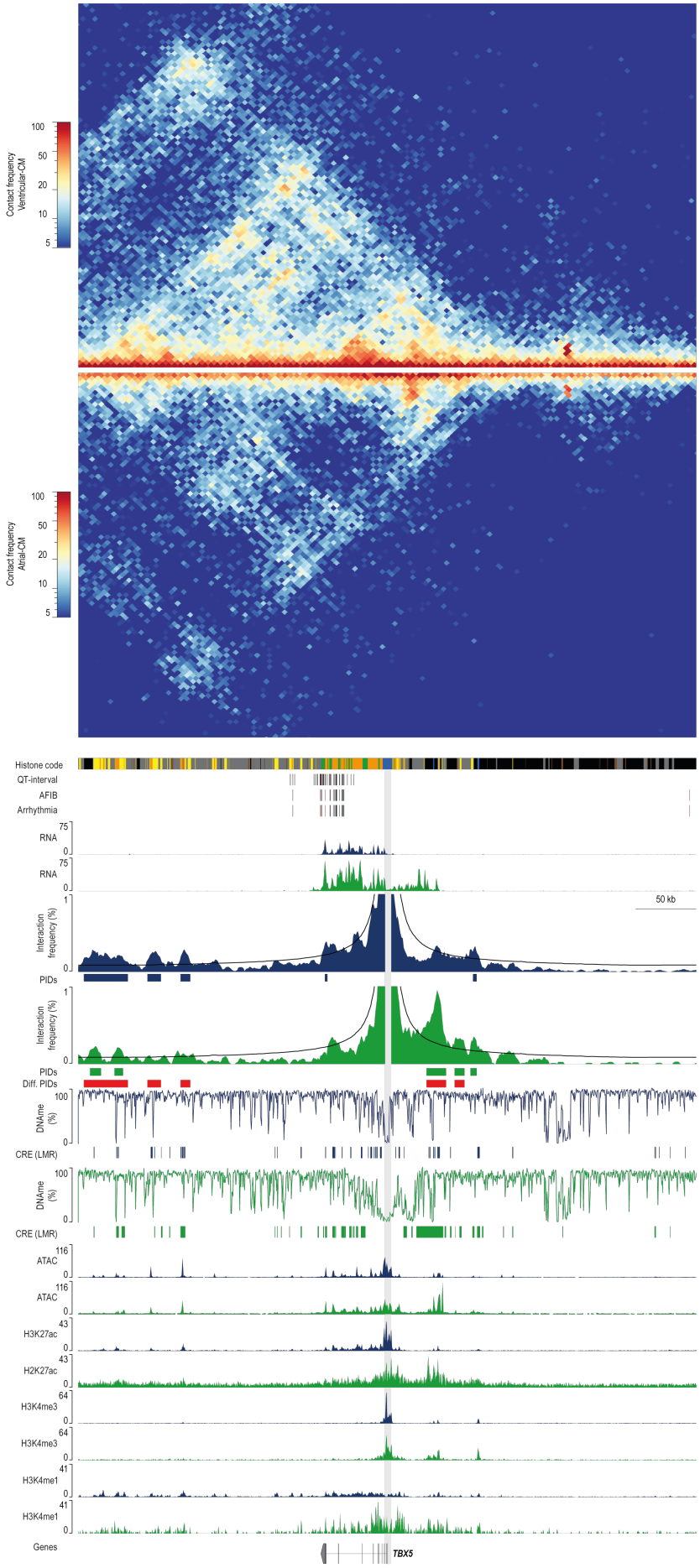
Contact frequency Ventricular-CM
100
50
20
10
5
Contact frequency Atrial-CM
100
50
20
10
5
Histone code
QT-interval
AFIB
Arrhythmia
RNA
75
0
RNA
75
0
50 kb
Interaction frequency (%)
1
0
PIDs
Interaction frequency (%)
1
0
PIDs
Diff. PIDs
DNAme (%)
100
0
CRE (LMR)
DNAme (%)
100
0
CRE (LMR)
ATAC
116
0
ATAC
116
0
H3K27ac
43
0
H2K27ac
43
0
H3K4me3
64
0
H3K4me3
64
0
H3K4me1
41
0
H3K4me1
41
0
Genes
TBX5

Supplementary Fig.13: Comparison of atrial and ventricular CM chromatin interactions for *TBX5* locus.
Original traces of and histone marks (ChromHMM), virtual viewpoint analysis of *TBX5* promoter interactions (Hi-C), mCpG (DNA methylation sequencing), gene expression (RNA-seq), chromatin accessibility (ATAC-seq), and histone modification (ChIP-seq). Low-methylated regions (LMR), PIDs, and differential PIDs are annotated. NF-LV-CM and NF-LA-CM tracks are shown in blue and green, respectively. Grey area highlights *TBX5* promoter. Hi-C data derived from *n* biological replicates: NF-LV-CM, 9; NF-LA-CM, 6. DNA methylation, histone modification ChIP-seq, and RNA-seq are reanalyzed from Gilsbach et al. 2018[1].

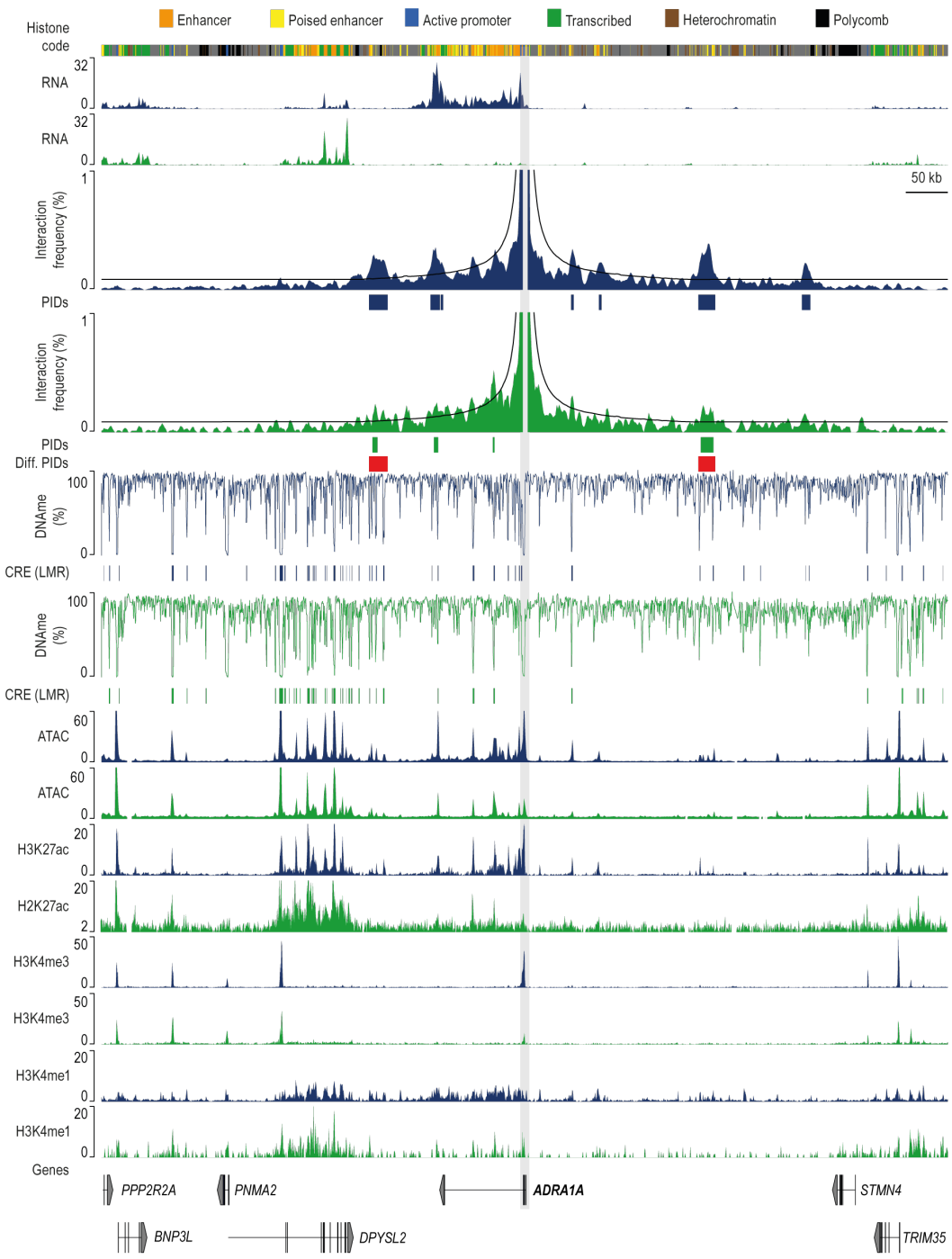

Supplementary Fig.14: Comparison of atrial and ventricular CM chromatin interactions for *ADRA1A* locus.
see legend Supplementary Fig. 13

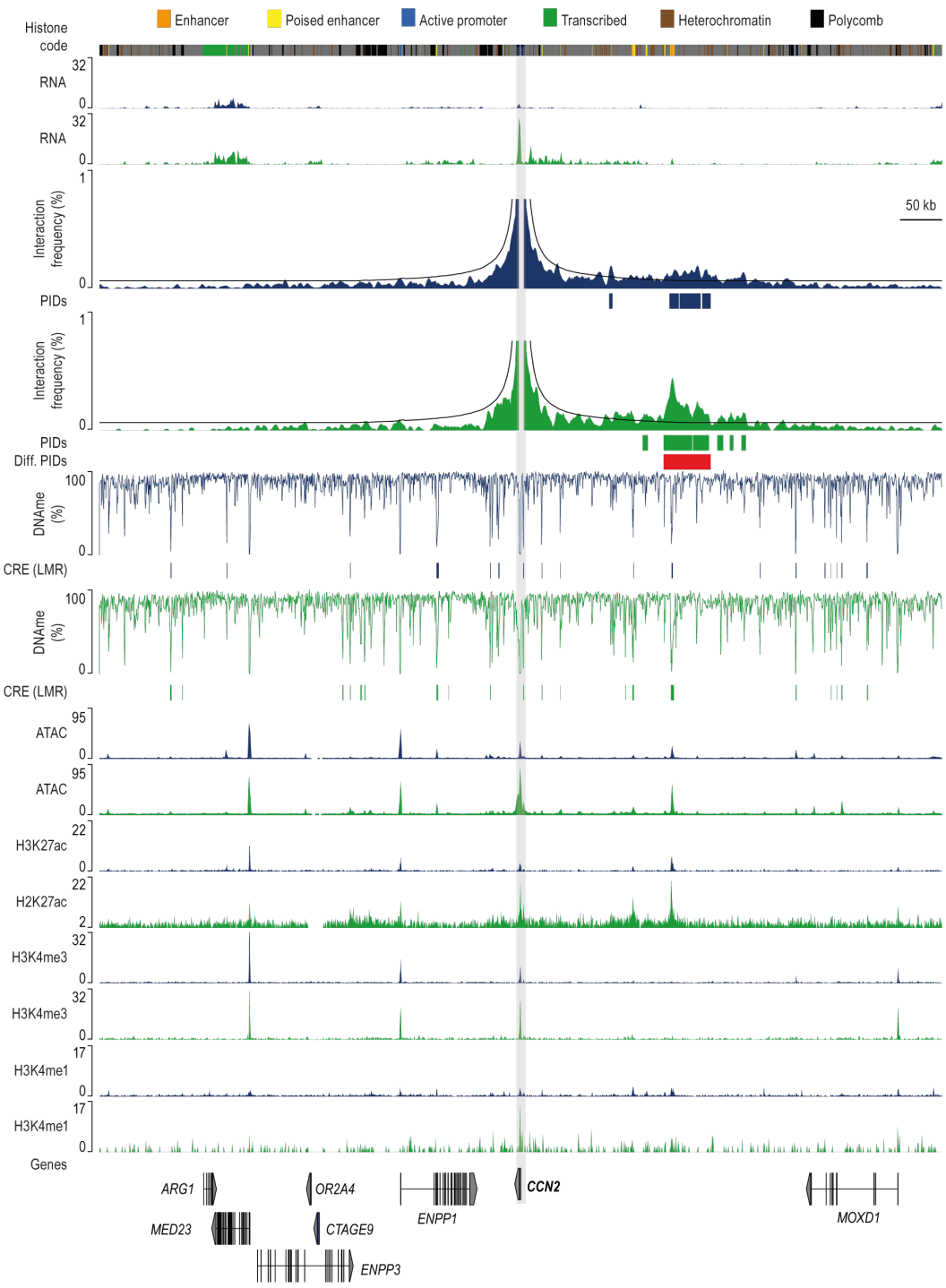

Supplementary Fig.15: Comparison of atrial and ventricular CM chromatin interactions for *CCN2* locus.
see legend Supplementary Fig. 13

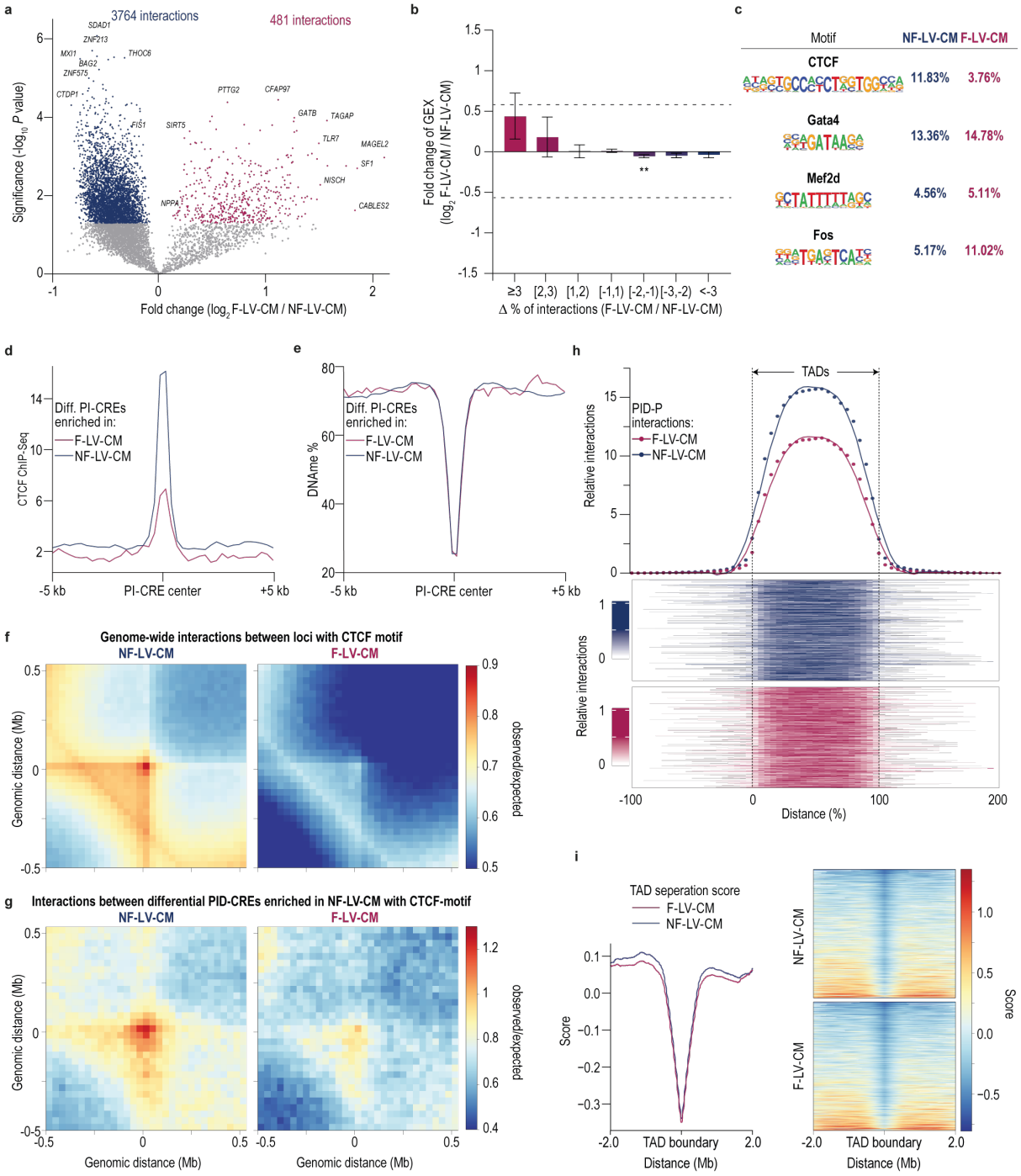

Supplementary Fig. 16: Comparison of chromatin interactions in non-failing and failing cardiomyocytes of the left ventricle.

a Volcano plot illustrating changes in promoter interacting domains (PIDs between NF-LV-CM and F-LV-CM. Differential PIDs were identified using a Chi-square test ($P < 0.05$), and a replicate-based post-hoc analysis was performed (T-test). Chromatin interactions with $P < 0.05$ are considered significant. Blue points indicate interactions significantly enriched in NF-LV-CM, while red points indicate those in F-LV-CM. Hi-C data derived from *n* biological replicates: NF-LV-CM, 9; F-LV-CM, 8.

b Bar plot showing the relationship between changes in promoter interactions and gene expression in NF-LV-CM versus F-LV-CM. Genes are categorized based on promoter interaction dynamics. Data presented as mean ± s.e.m. $^{**}P < 0.01$; $^{***}P < 0.001$; one-sample Wilcoxon signed rank test. GEX, gene expression.

c Transcription factor motif enrichment (%) in differential PI-CREs.

d Enrichment plot of CTCF is shown at differential PI-CREs between NF-LV-CM and F-LV-CM.

e Average mCpG metaplot of NF-LV-CM is shown at differential PI-CREs between NF-LV-CM and F-LV-CM.

f-g Contact frequency heatmaps centered on CTCF ChIP-seq peaks with convergent motif orientations, spanning a minimum of 50 kb to a maximum of 0.5 Mb (5 kb resolution).
Upper heatmaps show genome-wide CTCF interactions. Lower heatmaps represent interactions between differential promoter-interacting CREs enriched in NF-LV-CM with CTCF motif (Supplementary Fig. 16a, blue dots). Hi-C matrices were normalized to the lowest read count of the given matrices.
h Characterization of PID-promoter interactions in relation to their position within topologically-associated domains (TADs). The upper plot shows the sum of relative interactions. The lower heatmap represents the relative interaction in individual TADs. The intensity of blue and red horizontal lines represents the fraction of distal element-promoter interactions spanning the TAD locus in NF-LV-CM and F-LV-CM, respectively.
i Line plots and heatmaps show genome-wide insulation scores across the TAD boundaries of NF-LV-CM and F-LV-CM. TADs are calculated using a 50 kb resolution matrix.

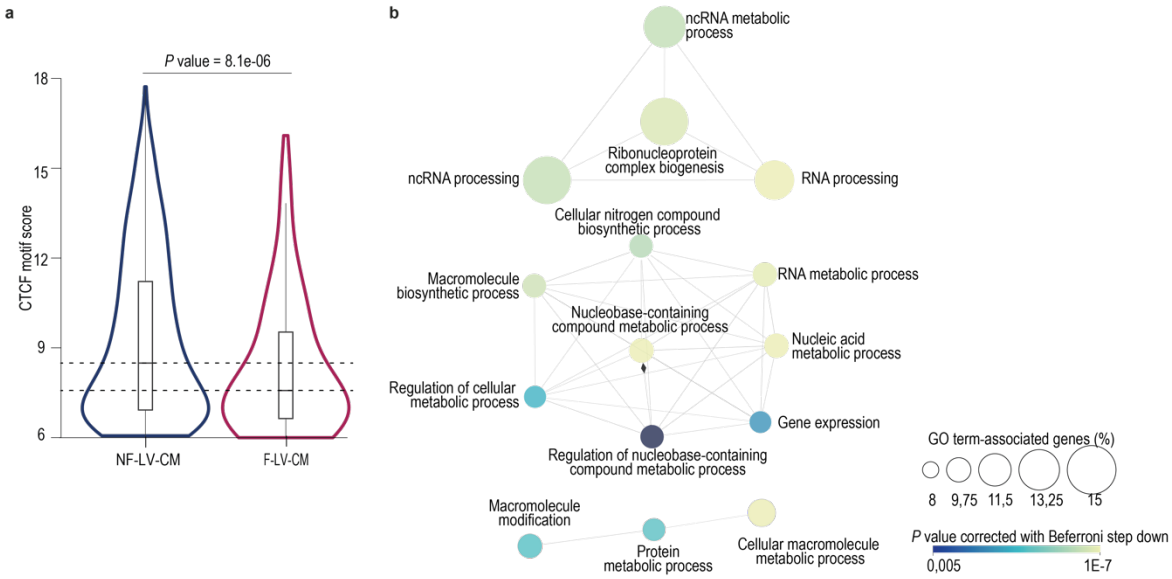

Supplementary Fig. 17: Characterization of differential PIDs of NF-LV-CM and F-LV-CM.
a Violin plots CTCF motif score of differential PIDs of NF-LV-CM and F-LV-CM.
b Gene ontology analysis of differential promoter interactions ($P < 0.01$) between NF-LV-CM and F-LV-CM. Significance threshold for calculating terms set at $P < 0.01$, Bonferroni step down correction.

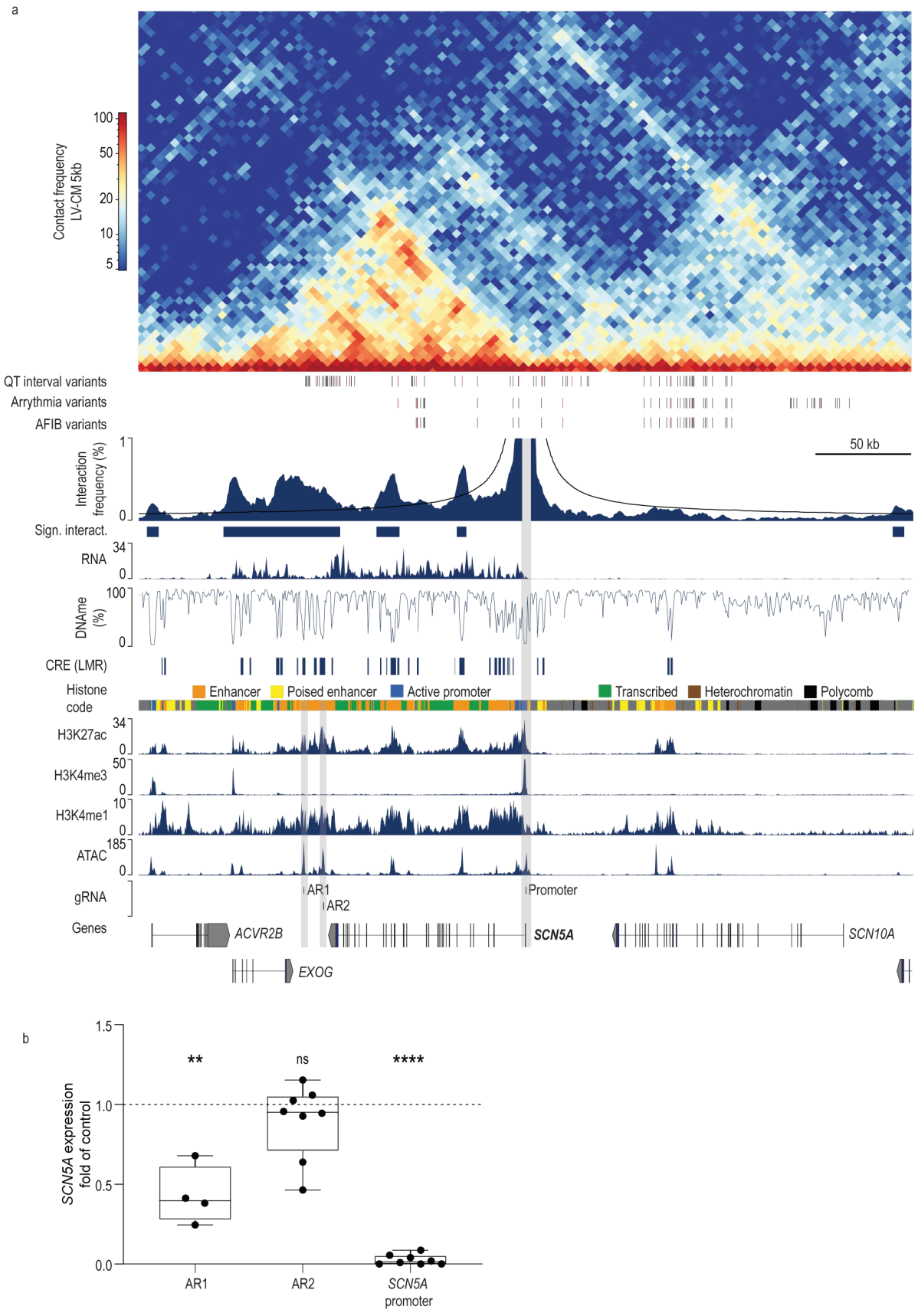

Supplementary Fig. 18: Functional relevance and promoter interactions of disease-associated non-coding variants in locus containing *SCN5A* gene.

a Heatmap of chromatin interactions (5 kb resolution) and GWAS variants for long QT syndrome, cardiac arrhythmia, and AFIB (lead-SNPs = red, proxy-SNPs = black). Virtual viewpoint analysis for the *SCN5A* promoter (1 kb resolution) and chromatin states are shown. Original traces for gene expression (RNA-seq), chromatin accessibility (ATAC-seq), and H3K27ac (ChIP-seq) of NF-LV-CM for genomic locus containing *SCN5A* are depicted. Hi-C data derived from 9 biological replicates. RNA-Seq and ATAC-Seq data are reanalyzed[1,2].
b CRISPRi silencing of two *SCN5A* promoter interacting elements (AR1 and AR2) and the *SCN5A* promoter. Lenti-transduced hiPSC-CM were FACS-sorted, and gene expression was measured by RT-qPCR. Grey areas in Supplementary Fig. 18a highlight the gRNA localization. *SCN5A* gene expression values are shown as box and whiskers (min to max) ($n \geq 4$). ns, $P \geq 0.05$; $^{**}P < 0.01$; $^{****}P < 0.0001$; One sample t-test.

References:

1 Gilsbach, R. *et al.* Distinct epigenetic programs regulate cardiac myocyte development and disease in the human heart in vivo. *Nat Commun* **9**, 391 (2018). https://doi.org/10.1038/s41467-017-02762-z

2 Zhang, M. *et al.* Long-range Pitx2c enhancer-promoter interactions prevent predisposition to atrial fibrillation. *Proc Natl Acad Sci U S A* **116**, 22692-22698 (2019). https://doi.org/10.1073/pnas.1907418116